Journal of Testing and Evaluation

doi:10.1520/JTE20160195 / Vol. 46 / No. 1 / January 2018 / available online at www.astm.org

H.-P. Lee,[1] A. Z. Awang,[2] W. Omar,[2] and P. L. Y. Tiong[3]

Derivation of Complete Stress–Strain Curve for SSTT-Confined High-Strength Concrete in Compression

Reference

Lee, H.-P., Awang, A. Z., Omar, W., and Tiong, P. L. Y., "Derivation of Complete Stress–Strain Curve for SSTT-Confined High-Strength Concrete in Compression," *Journal of Testing and Evaluation*, Vol. 46, No. 1, 2018, pp. 168–177, https://doi.org/10.1520/JTE20160195. ISSN 0090-3973

Manuscript received April 6, 2016; accepted for publication October 21, 2016; published online October 31, 2017.

[1] Dept. of Civil Engineering, Faculty of Engineering and QS (FEQS), INTI International Univ., Nilai, Negeri Sembilan 71800, Malaysia (Corresponding author), e-mail: leehoongpin@hotmail.com; hoongpin.lee@newinti.edu.my https://orcid.org/0000-0002-9122-1727

[2] Faculty of Civil Engineering, Universiti Teknologi Malaysia, UTM Skudai, Johor 81310, Malaysia

[3] School of Civil and Environmental Engineering, Nanyang Technological Univ., Singapore

ABSTRACT

For concrete structural behavior analysis, the complete axial stress–strain curves in compression can be determined by using a closed-loop servo-controlled hydraulic testing machine. The applied loading as well as the axial deformation reading of the loaded concrete specimen is recorded from the built-in displacement transducers or externally installed transducers placed between the machine platens. However, the recorded axial strain in the ascending branch is not purely concrete deformations but includes some additional deformation because of machine flexibility and specimen's end restraint. Strain gauges can be diametrically installed at the middle of specimen for a more precise deformation reading but additional costs are required for the gauges and data acquisition system. Moreover, the concrete stress–strain curve and ductility performance beyond its ultimate is difficult to be recorded without special strain measuring devices. Hence, a correction equation is needed to account for these effects to obtain the complete stress–strain curves for unconfined and confined concrete. In this paper, a total number of 84 unconfined and steel strapping tensioning techniques (SSTTs) confined high-strength concrete cylinders of compressive strength ranging from 62.48 MPa to 184.85 MPa were tested in compression in accordance with ASTM C39/C39M-11. The details for the testing setup, testing machine, strain measuring instruments, loading rate, loading patterns, etc. are described and at the same time a correction factor equation is proposed in this paper.

Keywords

Complete stress–strain relationship, uniaxial compression load test, correction factor derivation, high-strength concrete, steel strapping tensioning technique (SSTT)

Introduction

A complete stress–strain curve for unconfined and confined concrete is important for performance analysis and concrete structure design. It documents the overall response of the concrete structure from the

FIG. 1
The full volumetric ratio of SSTT-confined specimen.

beginning to failure under action of loading. It is quite a challenge to derivate the complete stress–strain curve under uniaxial compression because of two reasons: machine-specimen interaction and difficulty in measuring the actual concrete stains from the concrete specimen, especially upon reaching the ultimate compressive strength of the specimen.

Concrete's stress–strain relationship consists of two branches – an ascending and a descending branch. Ascending branch goes up to its ultimate stress and then followed by a descending branch until erratic deformation is observed or the compressive strength of concrete drops more than 50 % of its respective ultimate compressive strength, indicating failure of concrete. Testing machine with loading or deformation control can easily capture the ascending stress–strain deformation provided it measures the central region of the specimen using either electrical resistance strain gauges, or embedding steel bar to hold the transducers, or a compressometer. Recording the descending branch of the curve is the most difficult part of the experiment. Concrete starts to crack and deforms beyond the ultimate strength and these will damage the strain gauge or alter the contact point of the compressometer, resulting in erratic measurement, which do not representing the true deformation but false deformation. The accuracy of stress–strain relationship becomes particularly significant when dealing with high-strength concrete where high ductility is expected. Unconfined, high-strength concrete is relatively brittle and possesses lower ductility. However, the ductility increased when it is properly confined such as by fiber-reinforced polymer, concrete-filled tube, composite jacket, steel strapping tensioning technique, etc. [1–13]. Unless the compressive test is able to generate accurate and meaningful stress–strain curve, the ductility profile cannot be fully utilized.

Machine–specimen interaction is an accumulation of strain energy in the testing machine because of deformation of specimen and machine during the loading process. The energy is stored in the machine until the specimen reaches its ultimate capacity. The stored strain energy is then suddenly released as the concrete specimen has become weaker beyond its ultimate strength, leading to a sudden failure of the specimen. Such energy is relatively larger when dealing with high-strength concrete. Several solutions have been proposed to eliminate or reduce the interaction issue, e.g., control strain pace at a very low level to prevent sudden disintegration of the specimen and machine, or use steel cylinder in parallel with concrete test specimen to reduce the sudden release of strain energy from the machine during the entire test [14–21]. Nevertheless, even if the interaction problem was solved, the challenge in recording the descending branch of the stress–strain curve beyond the ultimate strength remains unsolved.

In addition, the whole surface of the confined concrete specimens was pre-tensioned with steel straps (**Fig. 1**) in this study, and it is impossible to install any strain gauge in the longitudinal direction especially in the center region to measure the strain level. Hence, to obtain an accurate, stable, and full stress–strain relationship, the concrete deformation values recorded between the machine platens during loading are generally used to compute the strain value in the stress–strain curve. Nevertheless, these calculated deformations are mixed with other unwanted strain values from the end-zone effect and residual deformation within the mechanical system of the machine. These values need to be isolated. In this paper, a correction factor is proposed to segregate those unwanted strain values so that more accurate stress–strain curves of unconfined and confined concrete can be obtained for the entire ascending and descending branches. Please note that the correction factor might vary depending on the type of testing machine, the method of specimen preparation, the loading pace and patterns, as well as the testing procedure.

Experimental Program

TEST SETUP AND STRAIN MEASURING INSTRUMENTATION

All of the compression tests were conducted using a TINIUS OLSEN Super "L" Universal Testing Machine, which has a capacity of 3 MN. Displacement-controlled loads were applied with a constant rate of 0.4 mm/min. The compression testing configuration is shown in **Fig. 2**.

The overall longitudinal axial deformations of the specimens were obtained using the three linear variable differential transducers (LVDTs) with gauge length of 50 mm, which were located at the machine platen. Another three LVDTs with a gauge length of 25 mm were attached to the center of the specimens with a longitudinal rig. The relative axial displacement was measure over the 100-mm height of the concrete specimens. The transverse deformations of the specimens were obtained using two separate LVDTs (gauge length of 25 mm) located at the center of the specimens, diametrically wrapped with steel ties around the concrete specimen. The overall concrete longitudinal strains were calculated from the average value from LVDT readings divided by the particular measured length.

The transverse deformations for concrete and steel strapping were obtained by using two sets of strain gauges (gauge length of 60 mm and 10 mm for concrete and steel strapping, respectively) installed at the center of the specimen in a diametrically opposed direction. Besides measurement values, visible observations such as crack pattern, buckling, and abnormal deformation were also carried out during the tests. The compressive strength of specimens was obtained in accordance to the testing procedures contained in ASTM C39/C39M-11 [1]. **Figs. 3** and **4** show the schematic diagram in detail for all measuring instruments used in this study, for both unconfined and confined concrete specimen, respectively. The only difference in measuring instruments between the two was the strain gauges to measure the lateral deformation of steel straps for confined concrete specimen.

LOADING PATTERNS—UNIAXIAL MONOTONIC LOADING TEST

In this study, the concrete specimens were tested under uniaxial monotonic loading tests to obtain their particular complete stress–strain relationship. Pre-load compression tests up to 10 % of the concrete's compressive strength have been carried out before the actual compression load test to eliminate the possibility of end-zone error. The loading pattern for this load test is shown in **Fig. 5**. The tests were performed until the compressive strength

FIG. 2

Strain measuring equipment (left) and the compression loading machine (right).

FIG. 3

Schematic diagram for unconfined specimen with its measuring instruments: (a) plan view, and (b) top view.

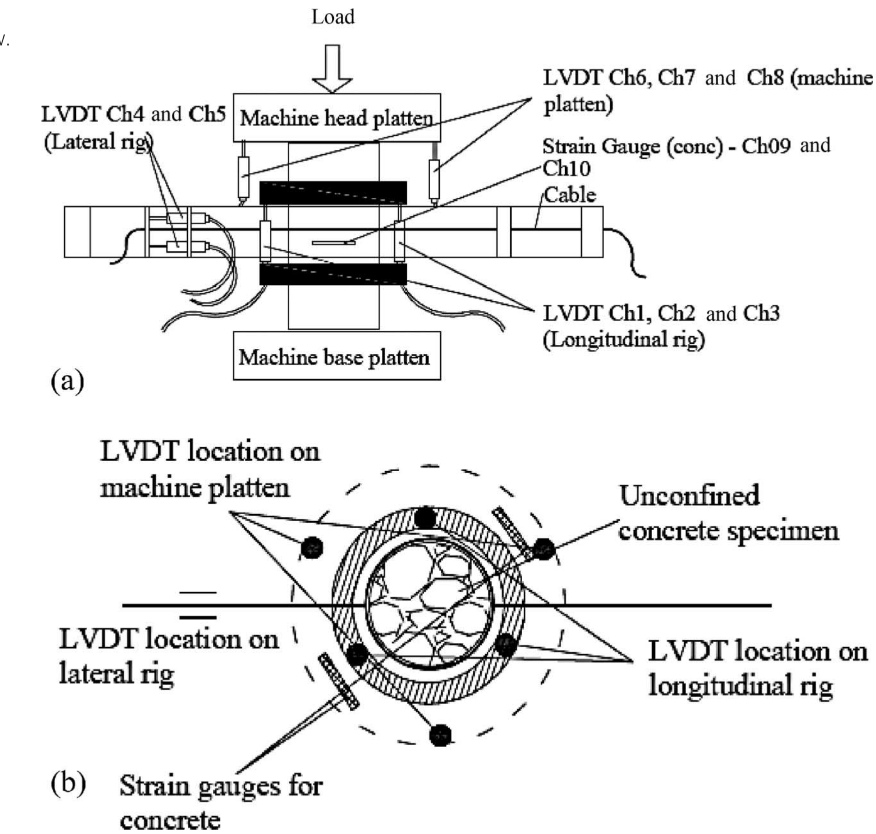

FIG. 4

Schematic diagram for confined specimen with its measuring instruments: (a) plan view, and (b) top view.

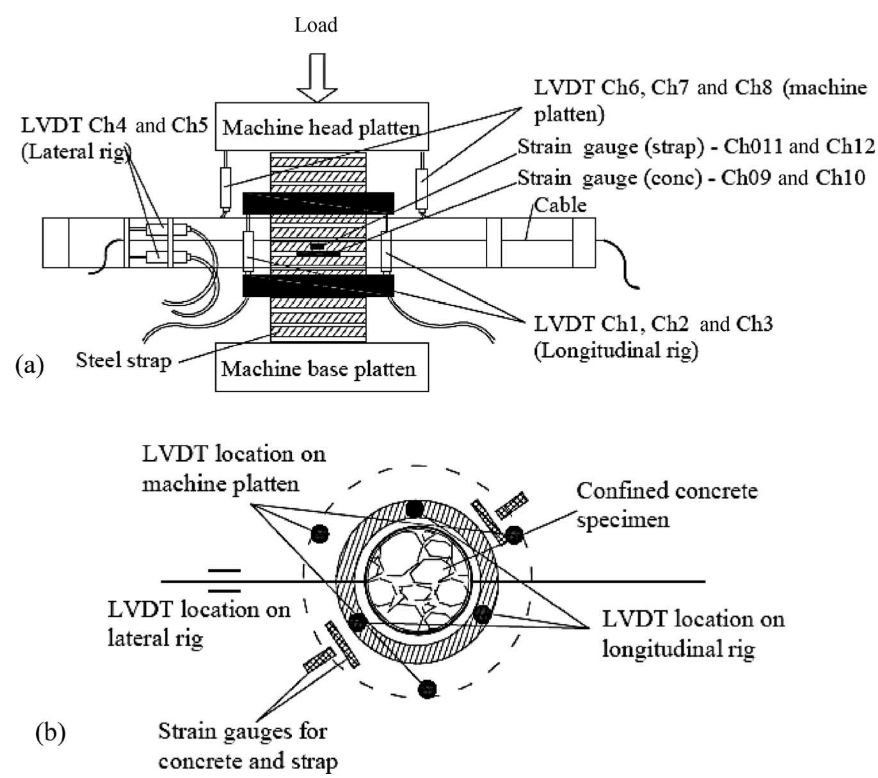

FIG. 5 Loading pattern for uniaxial monotonic loading text.

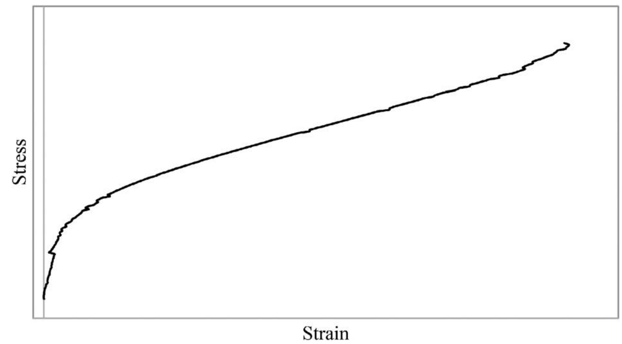

of loaded concrete specimens dropped by more than 50 % of its ultimate compressive strength. In some cases, the tests were stopped once erratic deformation was observed. Normally, erratic deformation happened in the post-peak region. Because such deformation does not represent the aspect of stress–strain behavior, the results were not counted. Some examples of erratic deformation obtained during the load test are shown in **Fig. 6**.

Derivation of Complete Stress–Strain Curve

To minimize the machine–specimen interaction as well as the disturbance from cracking while at the same time recording both ascending and descending branches of complete stress–strain curves, deformation of the concrete specimen between the machine platens were used to measure the concrete strains. This type of concrete strain is generally more reliable in the post-peak level but it does not fully represent the true strains of the specimen. The measured strain values included the unwanted end-zone effects and machine flexibility as per Mansur et al. [14]. These effects depended on the type of machine used, the method of preparation of the concrete specimen, testing procedure, and type of strain measuring technique. A correction factor (Eq 1) has been successfully proposed by Mansur et al. [14] to eliminate the unwanted effects for unconfined high-strength concrete with compressive strengths ranging from 50 to 130 MPa. It is also believed that there is a different in correction factor for both unconfined and confined concrete specimens, where a confined concrete specimen is the main objective of this study.

FIG. 6
Examples of erratic deformation for loaded concrete specimen (a to f).

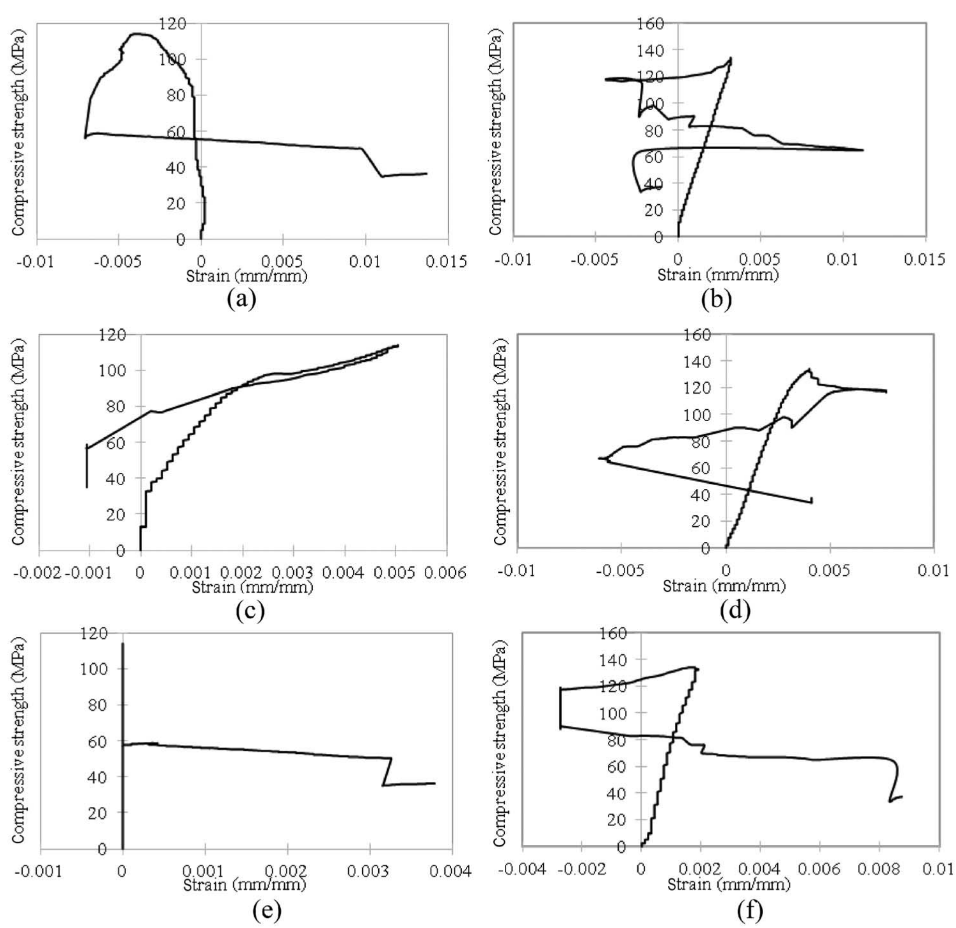

$$\alpha = \frac{229}{f_c} + 2.91 \tag{1}$$

TEST PROCEDURE FOR CORRECTION FACTOR

As the investigation for correction factor for the compression testing machine is a part of the investigation of the stress–strain behavior of unconfined and confined high-strength concrete in this study, a total number of 84 unconfined and SSTT confined high-strength concretes in the standard cylinders with dimensions of 100×200 mm and 150×300 mm were compressively tested using a TINIUS OLSEN Super "L" Universal Testing Machine. The design compressive strength of the unconfined concrete specimens were in the range of 65 to 107 MPa, whereas the compressive strength and confining ratio for the confined concrete specimens ranged from 63 to 185 MPa and 0.12 to 0.41 MPa, respectively. It is worth mentioning that the effect of cyclical loading was not included in this study. The compression test only utilized uniaxial monotonic loading in the vertical direction.

PRELIMINARY TEST RESULT AND THE NEED FOR CORRECTION

The LVDT rig used in this study had a fixed gauge length of about 95 mm for both types of standard cylinders (see **Fig. 7**); hence, the strain deformations obtained might probably contain some end-zone effects of the concrete specimen. To check the validity of the LVDT rig, unconfined concrete specimens of compressive strength of about 65 MPa and 110 MPa were installed with two sets of strain gauges with a gauge length of 60 mm in longitudinal direction, LVDT rig, and LVDT between the machine platens and tested with the uniaxial monotonic loading test until failure (**Fig. 7**). The stress–strain relationships derived from these two sets of deformations are shown in **Fig. 9** and **Fig. 10**.

The experimental results show that the two set of deformations measured are almost identical up to the peak load level for both the strain gauges and LVDT holder rig. The gauge length and the type of measuring instruments used in this study do not have a significant influence on the deformations. Hence, it can be concluded that the deformation of concrete specimens at the middle region has a no end-zone effect. Because of the difficulty of using a strain gauge in the longitudinal direction for SSTT-confined concrete specimens, it was therefore only the LVDT rig that was used to measure the actual deformation of the confined specimens. It should be noted that deformations obtained by strain gauges and LVDT rigs are only validated until the peak load level, where erratic deformations were significantly observed beyond the post-peak level after cracking began to occur.

To capture the descending branch of the stress–strain relationship of the concrete specimen, LVDTs that were placed between the machine platens (see **Fig. 8**) were used. The stress–strain relationship, recorded using the LVDTs between machine platens, has also been compared with the curves recorded by LVDT rig, as shown in **Figs. 9** and **10**. A significant difference exists between the two curves at all stress levels, whereby a constant difference in the gradient has been noticed. Hence, there is a relationship between the mentioned constant and concrete strength. This relationship is the so-called correction factor that needs to be implemented in

FIG. 7 The LVDT rig used to measure the middle half of the concrete specimen.

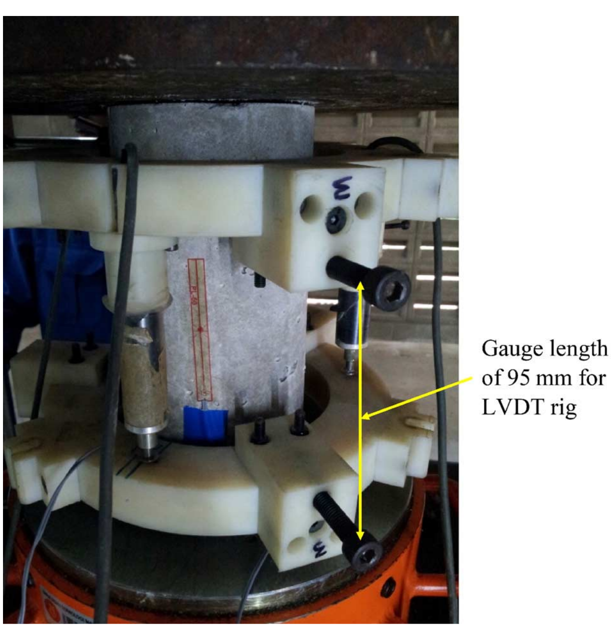

FIG. 8 Location of LVDT between machine platens.

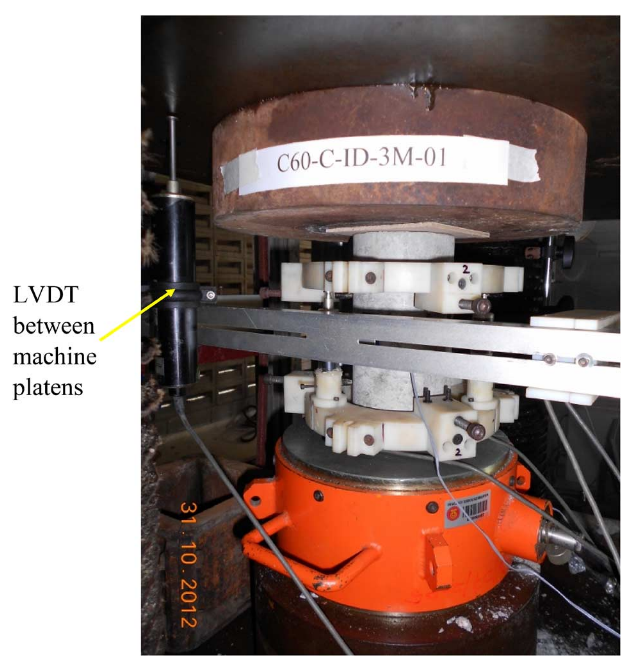

FIG. 9 Stress–strain curves from various measurement instruments (unconfined concrete specimen of compressive strength 65 MPa).

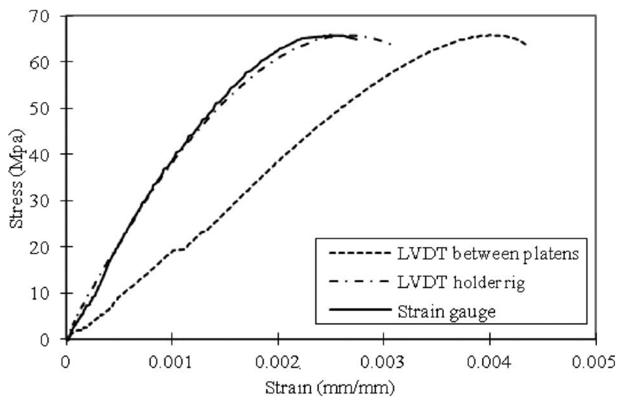

FIG. 10 Stress–strain curves from various measurement instruments (unconfined concrete specimen of compressive strength 110 MPa).

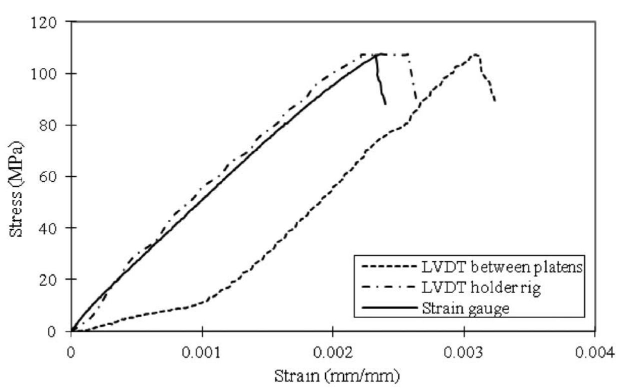

all of the stress–strain curves obtained by LVDT between machine platens.

DERIVATION OF CORRECTION FACTOR

Because there is a significant difference between the stress–strain curves obtained by the LVDT rig and LVDT in the middle of machine platens, a general factor was derived by Mansur et al. [14] in their paper using Eq 2. The correction factor is (α) comprised of initial tangent moduli of the concrete specimen based on the stress–strain curves derived from the LVDT rig and LVDT between machine platens in this study, as shown in **Fig. 11**. The inclusion of the correction factor in the deformation measured by LVDT between machines platens will give the corrected deformation similar to those measured by LVDT rig or strain gauges.

FIG. 11 Example case of initial tangent moduli derived from LVDT rig and LVDT between machine platens.

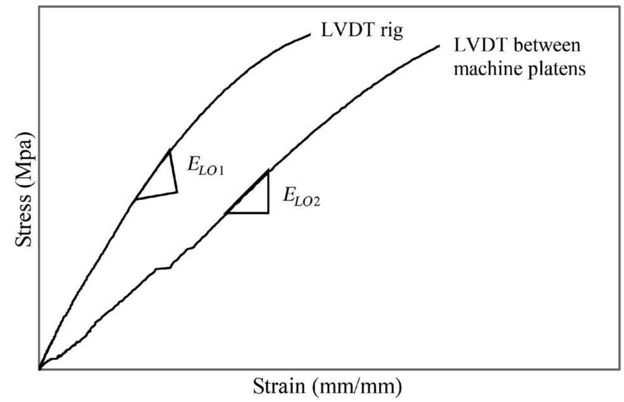

$$\alpha = \frac{1}{E_{LO2}} - \frac{1}{E_{LO1}} \tag{2}$$

The derivations for the correction factor are described below. Let Δ_{LO1} = deformation measured by LVDT rig over its gauge length, L_{rig}, Δ_{LO2} = deformation measured by LVDT between machine platens over its gauge length, L_P, Δ_a = the deformation because of machine flexibility and end-zone effect. The general deformation follows that:

$$\Delta_{LO2} = \Delta_{LO1} + \Delta_a \tag{3}$$

Rearranging Eq 3,

$$\Delta_a = \Delta_{LO2} - \Delta_{LO1} \tag{4}$$

The common equation for initial tangent moduli and strain,

$$E = \frac{\sigma}{\varepsilon} \tag{5}$$

and

$$\varepsilon = \frac{\Delta'}{L'} \tag{6}$$

where:

E = young modulus of concrete specimen,
σ = stress applied,
ε = strain deformation of concrete specimen,
Δ' = corresponding deformation measured by LVDT, and
L' = gauge length of the corresponding measuring instrument.

By substituting Eq 6 to Eq 5, we get,

$$E = \frac{\sigma}{\Delta'/L'} = \frac{\sigma L'}{\Delta'} \tag{7}$$

Rearranging Eq 7,

$$\Delta' = \frac{\sigma L'}{E} \tag{8}$$

Substituting Eq 8 into Eq 4, for its corresponding deformations measured by both measuring instruments, we get:

$$\Delta_a = \frac{\sigma L_P}{E_{LO2}} - \frac{\sigma L_{\mathrm{rig}}}{E_{LO1}} \tag{9}$$

Assume that $L_p = L_{\mathrm{rig}}$ as the strain difference is negligible compared to the length of the gauge; hence, we get:

$$\Delta_a = \left(\frac{\sigma}{E_{LO2}} - \frac{\sigma}{E_{LO1}}\right) L_P \tag{10}$$

Substitute Eq 10 into Eq 4 to replace the deformation Δ_a:

$$\Delta_{LO2} = \Delta_{LO1} + \left(\frac{\sigma}{E_{LO2}} - \frac{\sigma}{E_{LO1}}\right) L_P \tag{11}$$

By changing the deformation of concrete specimen to strain values, we get:

$$\varepsilon_{LO1} = \varepsilon_{LO2} - \left(\frac{1}{E_{LO2}} - \frac{1}{E_{LO1}}\right) \sigma \tag{12}$$

By substituting the parameters in the parentheses with the correction factor as described in Eq 2, we get:

$$\varepsilon_{LO1} = \varepsilon_{LO2} - (\alpha)\sigma \tag{13}$$

where:

ε_{LO1} = the newly corrected concrete strain at any stress level of σ, and

ε_{LO2} = the corresponding strain measured by LVDT between machine platens,

and the quantity in the parentheses in Eq 12 is the correction factor (α) used to revise the deformation from the machine platens. It is believe that concrete strength will have influence on the correction factor; hence, a correction factor relates to concrete strength, representing the correction factor proposed and described in the next section.

CORRECTION FACTOR

In an attempt to figure out a correction factor that can be generally used on the testing machine in Universiti Teknologi Malaysia so as to avoid the excessive use of the LVDT rig and to obtain both the ascending and descending branches of a concrete specimen without any erratic deformation, the correction factors obtained for each individual test are plotted against its corresponding compressive strength, as shown in **Fig. 12**. The curve indicates that the correction factor becomes smaller as the compressive strength of concrete increases. This might be because the small lateral dilation of higher strength concrete compared to the lower strength concrete at the same applied loading leads to smaller deformation between the platens on which the LVDTs are installed, and hence results in smaller correction factor. The scattering test results are acceptable because such differences are normal when dealing with concrete specimens with a high range of compressive strength. The best-fit curve for the range of concrete strength covered in this study can be expressed as in Eq 13, where the correction factor ranges from 4×10^{-6}/MPa to 11×10^{-6}/MPa for a variation of concrete strength from 60 MPa to 185 MPa:

FIG. 12 Relationship between correction factor and concrete compressive strength.

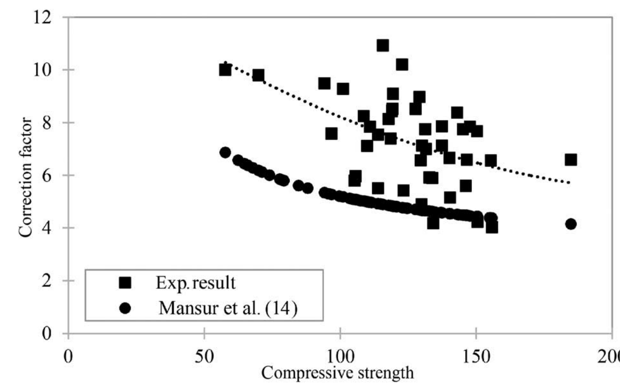

$$\alpha = 0.0002 f_c - 0.0946 f_c + 15.447 \tag{14}$$

where:

α = the correction factor that is only valid in the testing machine at the Faculty of Civil Engineering, Universiti Teknologi Malaysia, and

f_c = the compressive strength of corresponding concrete specimens based on either 100×200 mm cylinders or 150×300 mm cylinders, for both unconfined and confined concrete specimens.

In the same graph, the correction factor proposed by Mansur et al. is also included for comparison purposes. Mansur et al. investigates the correction factor for unconfined concrete specimens (standard concrete cylinders and concrete prisms) with compressive strength ranges from 50 MPa to 130 MPa, whereas the current study investigates the unconfined and confined concrete specimens (standard concrete cylinders) using SSTT confinement, with the compressive strength ranging from 60 MPa to 185 MPa. For a similar compressive strength, it is notified that the gradient of both curves are almost the same but the curve for current study is much higher than existing ones. Mansur et al.'s correction factor is mainly applicable to unconfined concrete only but the current proposed correction factor is feasible for both unconfined and confined concrete, exaggerating the application of

FIG. 13 Uncorrected and corrected stress–strain curves.

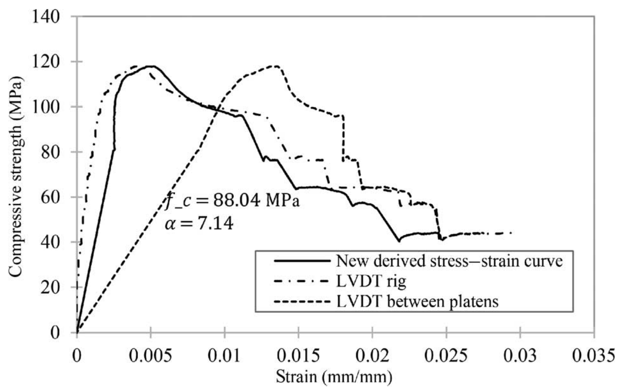

the correction factor. However, the correction factor would vary depending on the type of testing machine, the method of specimen preparation, the loading pace, loading patterns, and the overall testing procedure.

Fig. 13 shows the stress–strain curve for an SSTT confined concrete that has been corrected by using the proposed correction factor α, as derived above for the universal testing machine. It can be found that the unwanted extra deformation of LVDT between machine platens has been minimized and the corrected curve is closed to the true deformation of the concrete specimen. For the entire set of testing data that needed to be corrected in this study, it was concluded that the maximum deviation between the corrected curve and the actual curve was less than 10 %. Such a disparity occurs because of the unexpected pre-matured minor cracking error and other non-linearity in the end-zone effect. Therefore, it can be concluded that the correction factor proposed in this study is feasible for the particular universal testing machine in which an actual stress–strain curve could be obtained by regulating the strain value obtained by the deformation of machine platens using the proposed correction factor. By doing so, both actual longitudinal and lateral deformation of any types of confined concrete could be investigated without the use of any strain gauges and compressometer. This can save a certain amount of the budget on strain-measuring devices.

Conclusions

In this study, a total of 84 unconfined and SSTT-confined high-strength concrete cylinders with compressive strengths ranging from 62.48 MPa to 184.85 MPa with dimensions 100 mm × 200 mm and 150 mm × 300 mm in diameter and height, respectively, were compressively tested with a prescribed strain-measuring method. The results demonstrated that, by using LVDT rigs fixed directly to the concrete specimen and LVDT placed between the machine platens, a correction factor to segregate the machine flexibility and end-zone effect can be determined. By applying the correction factor, a near-to-actual stress–strain curve of unconfined or confined concrete in compression can be obtained without relying on strain gauges or a compressometer. It should be noted that the above conclusions have been reached only in regard to the laboratory tests conducted on standard, scaled, high-strength concrete specimens at the Faculty of Civil Engineering, Universiti Teknologi Malaysia. Correction factors would vary depending on the type of testing machine, the method of specimen preparation, the loading pace, loading patterns, and the overall testing procedure.

ACKNOWLEDGMENTS

The work described in this paper is supported by the GUP Grant (Tier1) of Universiti Teknologi Malaysia (No. QJ13000.2522.09H34) and INTI International University Grant (No. INT-FOSTEM-02-01-2015). The authors are also grateful to Mybrain15 from the Ministry of Higher Education of Malaysia for sponsoring this research study through the MyPhd scholarship. Laboratory testing of the concrete specimens was performed in the Laboratory of Structural Engineering of Universiti Teknologi, Malaysia. Assistance from the dutiful technicians are very much acknowledged.

References

[1] ASTM C39/C39M-11, *Standard Test Method for Compressive Strength of Cylindrical Concrete Specimens*, ASTM International, West Conshohocken, PA, 2011, www.astm.org
[2] Awang, A. Z., "Stress-Strain Behaviour of High-Strength Concrete with Lateral Pre-Tensioning Confinement," Universiti Teknologi, Malaysia, 2013.
[3] Awang, A. Z., Omar, W., and Hoong-Pin, L., "The Effectiveness of Metal Straps Strengthening in Layers at High Strength Concrete Column," *APSEC-ICCER 2012*, Surabaya, Indonesia, 2–4 Oct 2012; University of Technology, Malaysia, Hotel Mercure, Surabaya, Indonesia.
[4] Awang, A. Z., Omar, W., Hoong-Pin, L., and Ma, C. K., "Behaviour of Externally Confined High Strength Concrete Column Under Uniaxial Compression Load," *APSEC-ICCER 2012*, Surabaya, Indonesia, 2–4 Oct 2012; University of Technology, Malaysia, Hotel Mercure, Surabaya, Indonesia.
[5] Benzaid, B., Chikh, N. E., and Mesbah, H., "Study of the Compressive Behaviour of Short Concrete Columns Confined by Fibre Reinforced Composite," *Arab. J. Sci. Eng.*, Vol. 34, No. 1, 2009, pp. 15–26.
[6] Benzaid, R., Chikh, N. E., and Mesbah, H., "Behaviour of Square Concrete Column Confined with GFRP Composite Warp," *J. Civ. Eng. Manage.*, Vol. 14, No. 2, 2008, pp. 115–120, https://doi.org/10.3846/1392-3730.2008.14.6
[7] Berthet, J. F., Ferrier, E., and Hamelin, P., "Compressive Behaviour of Concrete Externally Confined by Composite Jackets. Part A: Experimental Study," *Constr. Build.*

Mater., Vol. 19, No. 3, 2005, pp. 223–232, https://doi.org/10.1016/j.conbuildmat.2004.05.012

[8] Hong, K. N., Han, S. H., and Yi, S. T., "High-Strength Concrete Columns Confined by Low-Volumetric-Ratio Lateral Ties," *Eng. Struct.*, Vol. 28, No. 9, 2006, pp. 1346–1353, https://doi.org/10.1016/j.engstruct.2006.01.010

[9] Hoong-Pin, L., Awang, A. Z., and Omar, W., "Behaviour of Steel Strapping Tensioning Technique (SSTT) Confined High-Strength Concrete with Different Lateral Pre-Tensioning Stresses," *IGCESH 2013*, Malaysia, 16–17 April 2013, University of Technology, Malaysia, SPS, University of Technology, Malaysia.

[10] Hoong-Pin, L., Awang, A. Z., and Omar, W., "Strength and Ductility of High-Strength Concrete Cylinders Externally Confined with Steel Strapping Tensioning Technique (SSTT)," *J. Teknol.*, Vol. 68, No. 1, 2014, pp. 109–118.

[11] Hoong-Pin, L., Awang, A. Z., and Omar, W., "Steel Strap Confined High Strength Concrete under Uniaxial Cyclic Compression," *Constr. Build. Mater.*, Vol. 72, 2014, pp. 48–55, https://doi.org/10.1016/j.conbuildmat.2014.08.007

[12] Issa, M. A. and Tobaa, H., "Strength and Ductility Enhancement in High-Strength Confined Concrete," *Mag. Concr. Res.*, Vol. 46, No. 168, 1994, pp. 177–189, https://doi.org/10.1680/macr.1994.46.168.177

[13] Lambert, A. N. and Tabsh, S. W., "Ductility Enhancement of High Strength Concrete Columns with Welded Wire Mesh," *Proceedings of Structures 2004: Building on the Past, Securing the Future*, Nashville, TN, May 22–26, 2004, ASCE, Reston VA.

[14] Mansur, M. A., Wee, T. H., and Chin, M. S., "Derivation of the Complete Stress–Strain Curves for Concrete in Compression," *Mag. Concr.*, Vol. 47, No. 173, 1995, pp. 285–290, https://doi.org/10.1680/macr.1995.47.173.285

[15] Mei, H., Kiousis, P. D., Ehsani, M. R., and Saadatmanesh, H., "Confinement Effect on High-Strength Concrete," *ACI Struct. J.*, Vol. 98, No. 4, 2001, pp. 548–553.

[16] Nisnevich, M., Sirotin, G., and Belostozky, B., "Improving Mechanical Characteristics of High-Strength Concrete Under Confining Effect by Loading," *The Research Institute of the College of Judea and Samaria*, Ariel, Israel, 2008.

[17] Ros, P. S., Yazzar, S. A., and Calvo, A. C., "Influence of Confinement on High Strength Concrete Behaviour," *Mater. Struct.*, Vol. 36, No. 439, 2003, pp. 439–447, https://doi.org/10.1007/BF02481523

[18] Rousakis, T. C., "Experimental Investigation of Concrete Cylinders Confined by Carbon FRP Sheets, Under Monotonic and Cyclic Axial Compressive Load," Demokritus University of Thrace, Komotini, Greece, 2001.

[19] Sharma, U. K., Bhargava, P., and Kaushik, S. K., "Behaviour of Confined High Strength Concrete Columns Under Axial Compression," *J. Adv. Concr. Technol.*, Vol. 3, 2005, pp. 267–281, https://doi.org/10.3151/jact.3.267

[20] Valdmanis, V., Lorenzis, L. D., Rousakis, T., and Tepfers, R., "Behaviour and Capacity of CFRP-confined Concrete Cylinders Subjected to Monotonic and Cyclic Axial Compressive Load," *Struct. Concr.*, Vol. 11, No. 4, 2007, pp. 187–200.

[21] Yong, Y. K., Nour, M. G., and Nawy, E. G., "Behaviour of Laterally Confined High-Strength Concrete Column Under Axial Loads," *J. Struct. Eng.*, Vol. 114, No. 2, 1988, pp. 332–351, https://doi.org/10.1061/(ASCE)0733-9445(1988)114:2(332)